PRECISION MEASUREMENT OF MUON G-2 AND ACCELERATOR RELATED ISSUES*

H. N. Brown[2], G. Bunce[2], R. M. Carey[1], P. Cushman[9], G. T .Danby[2], P. T. Debevec[7], M. Deile[11], H. Deng[11], W. Deninger[7], S. K. Dhawan[11], V. P. Druzhinin[3], L. Duong[9], E. Efstathiadis[1], F. J. M. Farley[11], G. V. Fedotovich[3], S. Giron[9], F. Gray[7], D. Grigoriev[3], M. Grosse-Perdekamp[11], A. Grossmann[6], M. F. Hare[1], D. W. Hertzog[7], V. W. Hughes[11], M. Iwasaki[10], K. Jungmann[6], D. Kawall[11],M.Kawamura[10], B.I.Khazin[3], J.Kindem[9], F.Krienen[1], I.Kronkvist[9], R.Larsen[2], Y.Y.Lee[2], I.Logashenko[1,3], R.McNabb[9], W.Meng[2], J.Mi[2], J.P.Miller[1], W.M.Morse[2], D.Nikas[2], C.J.G.Onderwater[7], Y.Orlov[4], C.S.Ozben[2], J.M.Paley[1], C.Polly[7], J.Pretz[11], R.Prigl[2], G.zuPutlitz[6], S.I.Redin[11], 0.Rind[1], B.L.Roberts[1], N.Ryskulov[3], S.Sedykh[7], Y.K.Semertzidis[2], Yu.M.Shatunov[3], E.P.Sichtermann[11], E.Solodov[3], M.Sossong[7], A.Steinmetz[11], L.R.Sulak[1], C.Timmermans[9], A.Trofimov[1], D.Urner[7], P.vonWalter[6], D.Warburton[2], D.Winn[5], A.Yamamoto[8], D.Zimmerman[9]

*1)Department o f Physics, Boston University, Boston, MA*0 2215, *USA*
2)Brookhaven National Laboratory, Upton, NY 11973, *USA*
3)Budker Institute of Nuclear Physics, Novosibirsk, Russia
4)Neuman Laboratory, Cornell University ,Ithaca, NY 14853, *USA*
5)Fairfield University, Fairfield, CT 06430, *USA*
6)Physikalisches Institut der Universitat Heidelberg, 69120 *Heidelberg, Germany*
7)Department of Physics, University of Illinois at Urbana-Champaign, IL 61801, *USA*
8)KEK ,High Energy Accelerator Research Organization, Tsukuba, Ibaraki 305-0801, *Japan*
9)Department of Physics, University of Minnesota, Minneapolis, MN 55455, *USA*
10)Tokyo Institute of Technology, Tokyo, Japan
11)Department of Physics, Yale University, New Haven, CT 06520, *USA*

Abstract

A precision measurement of the anomalous *g* value, a_μ=(g-2)/2, for the positive muon has been made using high intensity protons available at the Brookhaven AGS. The result based on the 1999 data a_μ=11659202(14)(6)x 10^{10} (1.3ppm) is in good agreement with previous measurements and has an error one third that of the combined previous data. The current theoretical value from the standard model is a_μ (SM)= 11659159.6(6.7) x 10^{10} (0.57 ppm) and differ by over 2.5 standard deviation with experiment. Issues with reducing systematic errors and enhancing the injection and storage efficiencies are discussed.

1 INTRODUCTION

Precise muon g-2 measurements, when compared to precise theoretical predictions of known physics, gives insight to whether there are new physics contributions present such as Supersymmetry or W boson substructure to name a few. The original goal of the experiment was, and still is, to measure the value to a precision of 0.35 parts per million (ppm) compare to previous CERN measurement [1] of 7.3 ppm. This report is based on the 1999 data run of 1.3 ppm measurement, limited mainly by statistics. The experiment uses the same principle as the CERN but improved to reduce systematic errors and to enhance the statistics. The principle of the experiment, previous results on earlier data, and many experimental details have been given in earlier publications [2,3].

What we measure is the difference between muon spin precession and cyclotron frequency

$$\omega_a = \omega_s - \omega_c = \frac{eB}{mc}$$

where ω_s and ω_c are the muon spin precession and cyclotron frequencies and B is the magnetic field. In the storage ring of uniform magnetic field, one can observe the rotation frequency of the spin direction because the

* Work supported in part by US Dept of Energy, US NSF, German Bundesminister fur Buildung unt Forschung, Russian Ministry of Science, and US-Japan Agreement in High Energy Physics.

decay positron is preferentially in the direction of the muon spin in parity violating μ^+ decay. By observing positron with high enough energy to be in direction of muon motion one can measure the rotation frequency of the muon spin.

The muon storage ring consists of uniform magnetic dipole guide field and focusing provided by electrostatic quadrupoles. The quantity ω_a is independent of electrostatic field at so called magic momentum of γ=29.3 or p_μ=3.094GeV/c. Therefore at this momentum one can use electrostatic quadrupoles insteads of magnetic gradient to focus the stored muon and avoid corresponding uncertainty in the magnetic field applicable to the muon population. Highly polarized muons of 3.094 GeV/c from decay of secondary pion beamline are injected through a superconducting inflector [4] into a storage ring 14.2 m in diameter with an effective circular aperture 9 cm in diameter. The superferric storage ring[5] has a homogeneous magnetic field of 1.45 T, which is measured by an NMR system relative to the free proton NMR frequency [6] . A pulsed magnetic kicker gives a 10 m-rad deflection which places the muons into stored orbits. Positrons are detected using 24 lead/scintillating fiber electromagnetic calorimeters [7] read out by waveform digitizers. The waveform digitizer and NMR clocks were phase-locked to the Loran C frequency signal. The muon of this energy has a lifetime of 64.4 μ-sec. in the laboratory frame. And we have been able to observe some 140 muon g-2 periods. In addition to 375 fixed NMR probes on top and bottom of the vacuum chamber monitoring the magnetic field continually, the field is monitored with the travelling NMR trolley with 17 probes inside the vacuum chamber mapping the field distribution often while data taking.

2 **STORAGE RING AND THE MAGNET**

The BNL g-2 storage ring was built as a single continuous magnet of homogeneous field of 1.45T superferric construction (an iron magnet excited by superconducting coils) guaranteeing azimuthal uniformity of the field. The vertical focusing is provided by electrostatic quadrupoles covering half the ring circumference. The focusing lattice has four fold symmetric structure to insure smooth batatron functions. Size variation of the stored beam is minimal throughout the ring as β_{max}/β_{min}=1.04. The muons are stored in a circular aperture of 9 cm diameter which is much smaller than magnet gap to insure a good field. Two of the empty spaces of the ring are occupied by injection inflector and the fast injection kickers. The plan view of the ring is shown in fig. 1. The magnet is C-shaped as dictated by the experiment requirement that decay electrons be observed inside the ring. The cross section of the magnet is shown in Fig 2**.** The use of superconducting coils offered the following advantages: thermal stability once cold; relatively low power requirements; low voltage, and hence use of a low voltage power supply; high L/R value and hence low ripple currents; and thermal independence of the coils and the iron. It is a goal of the experiment to produce a magnet of about 1 ppm uniformity over the muon storage aperture.

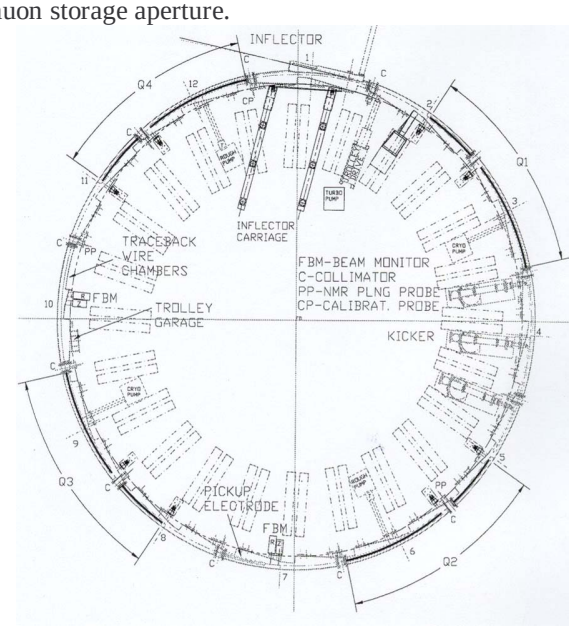

Fig. 1: Planview of the g-2 ring

The field, and hence its homogeneity and stability are determined dominantly by the geometry, characteristics, and construction tolerances of the iron.

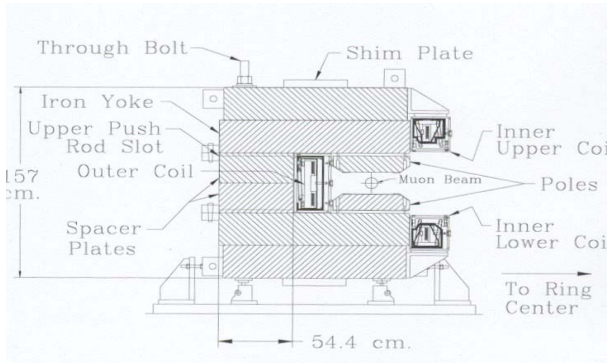

Fig.2: Cross section view of the magnet

The NMR measurements give the additional factor of 10 improvement in knowledge of the field. The magnet is designed as a shimmable kit. Passive iron shimming is used to correct imperfections in the initial assembly by a factor of two or three orders of magnitude. Iron shimming includes adjustments to the yoke plates above and below the magnet shown in Fig 2**,** insertion of iron in the air gaps between the poles and yoke (Fig. 3), and adjustment of edge shims on the poles. Correcting coils on the surface of the poles permit ultimate control of static, cyclical, and even slowly varying errors. The surface coils can be used to correct lower multipoles to tens of ppm, so that significant overlap shimming exists between planned iron shimming and the surface coils.

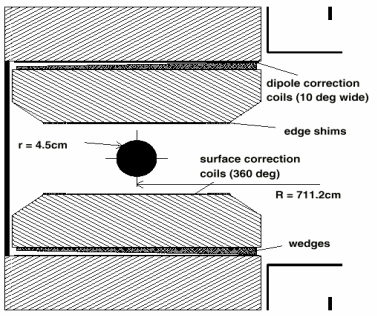

Fig 3: Cross section view of magnet gap region

The air gap between each pole piece and the top and bottom plates, respectively, of the yoke (Fig 3) serves to decouple the storage region precision field shape from the impact of variations within normal tolerances of yoke piece magnetic properties and mechanical dimensions. This decoupling of the yoke also desensitizes the impact of major yoke perturbations, principally the large hole for the entering beam and holes in the yoke for the coil transfer lines. Additional steel was added adjacent to these holes to restore the reluctance to its unperturbed value.

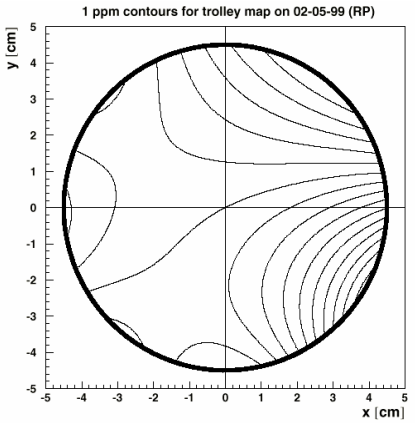

Fig 4: Two dimensional field multipole expansion of a typical trolley measurement during 1999 data taking. Contours are steps of 1 ppm respect to central average field of 1.451266T. The perimeter circle indicates the storage ring aperture.

The magnetic field B is measured and monitored by NMR measurements of the free proton resonance frequency ω_p. In addition to the 375 fixed NMR probes mounted on the top and the bottom of the vacuum chamber throughout the ring, seventeen NMR probes are mounted in an array on a trolley which moves on a fixed track inside the muon storage ring vacuum. The trolley probes are calibrated with respect to a standard spherical H_2O probe to an accuracy of 0.2 ppm before and after data-taking periods. Interpolation of the field in the periods between trolley measurements, which are made on average every three days, is based on the readings of about 150 fixed NMR probes distributed around the ring in the top and bottom walls of the vacuum chamber. Fig. 4 shows a magnetic field profile averaged over azimuth. The variations in the amplitudes of the multipoles affect (B) by less than 0.02 ppm. The average readings of 36 uniformly distributed fixed probes are maintained to 0.1 ppm by feedback to the main magnet power supply. Table 1 is a summary of the magnetic field contribution to the systematic error for g-2 measurement .

Table 1:
Systematic error for ω_p for 1999 run

	ppm
Absolute Calibration	0.05
Trolley Probe Calibration	0.20
Trolley Measurement of B_o	0.10
Interpolation With Fixed Probe	0.15
Inflector Fringe Field	0.20
Muon Distribution Uncertainty	0.12
Miscellaneous	0.15
Total Systematic	0.4

Miscellaneous items include uncertainty of remnant eddy current field from the injection kickers. In 1999 run we had a gap in the inflector superconducting shield which accounts for majority of the inflector fringe field. The problem has been corrected for later runs in 2000 and 2001. The result of 2000 runs will be reported later this year.

3 INJECTION INFLECTOR

The inflection of particle beam into a storage ring is usually done with a pulsed magnetic inflector, which cancels the field of the ring magnetic field, so that the beam enters the storage region as close as possible, and tangent to the equilibrium orbit. An injection kicker placed downstream will place the beam in the storage ring orbit. We have studied and discarded a pulsed option used in the CERN experiment because it would be difficult to accommodate the repetition rate of the experiment. Because of the stringent magnetic field requirement of the storage ring one should not introduce any magnetic material in to the ring. A none-ferrous DC double cosine theta septum[4], which contains magnetic flux entirely within the magnet, is chosen for this purpose. The cross section of the magnet is shown in fig. 5. The requirements for the DC inflector septum are to produce magnetic field of 1.5T over the length of 1.7m in order to cancel the integrated fringe field of the ring and to keep its stray field down low. The integrated fringe field is dominated by the end of the septum near the storage area, however the static nature of the fringe field enable shimming and precise measurement to apply corrections. Nevertheless, reducing the stray field as much as one can is important.

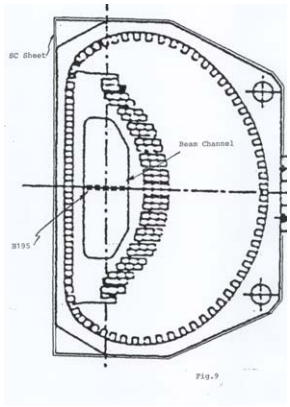

Fig. 5: None-ferrous superconducting setum with superconducting shield around.

By wrapping the inflector magnet with a superconducting sheet before turning the septum on will trap all magnetic flux inside the sheet and keep the storage region free of the stray field. The turn on procedure is to turn the main ring dipole on while the shield conductor is normal, and make the shield superconducting before the inflector septum turns on. In this way the main dipole field is inside the shield while stray field is excluded from the storage region. A typical test result is shown in the fig. 6. In 1999 run, we had a gap in the shield and the stray field was worse than we hoped for. The problem had been remedied for later runs.

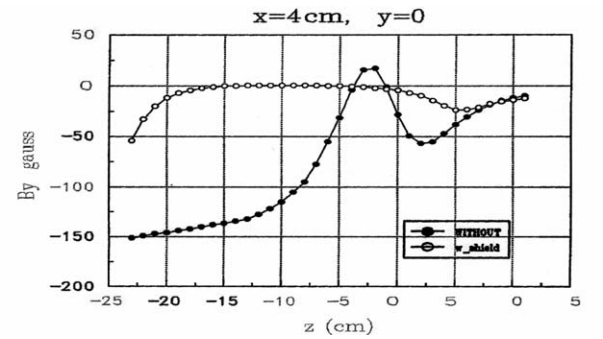

Fig. 6: Superconducting inflector shield test at 4cm from centre of storage region; open circle with shield and closed circle without. Z is distance along the inflector with 0 be the septum end.

4 MUON INJECTION AND INJECTION KICKER

Pion injection utilizes the muon decay angle as a kick required to be stored in the ring. There are two problems associated with pion injection. One is that the process is very inefficient; injection efficiency is about 20~30 ppm of injected pions. This raises another problem namely every unsuccessful pion may end up interacting with the vacuum chamber and the detectors. This initial flash at the detector creates a significant problem.

Direct muon injection is far more efficient in producing stored muons compared to pion injection by a factor of 10, and the hadronic background associated with many pions interacting with the storage ring material is greatly reduced. Although muons may accompany as many as twice the pions in muon injection, it is still orders of magnitude less than pion injection. Since the inflector brings the centre of injected muon to 76 mm from storage centre, one needs 10 m-rad kick about a quarter the circumference downstream. We used three modules of kicker current sheet of 1.7 m length producing a magnetic field to achieve this purpose. The cross sectional view of the kicker plate inside the vacuum chamber is shown Fig. 7. The kicker plate also serves as a rail for the NMR trolley. A cross section of NMR trolley is also shown.

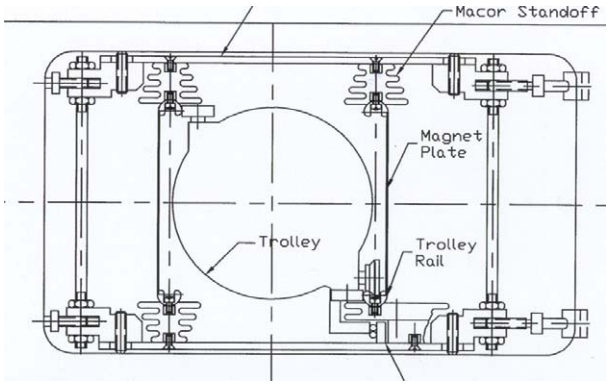

Fig. 7: Cross sectional view of the kicker and NMR trolley Inside the vacuum chamber

The rise and fall time of the kicker is nominally 200 n-sec mainly restricted by the availability of high voltage Pulse Forming Network (PFN). An injection efficiency of about 7% is achieved. Since the phase space acceptance of the storage ring and the inflector channel is different and not matched, resultant muon distribution is rather lumpy in the storage area, certain corrections are made to g-2.

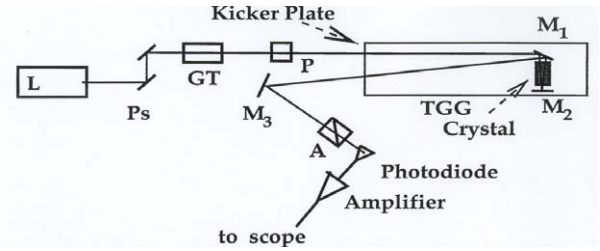

Fig. 8: Faraday effect experimental set up. L; laser, p_s; periscope, M; mirror, A; analyser, P; polarizer, GT; Galilean telescope

One persistent question was how much the remnant magnetic field of the kicker induced by the eddy current. We have measured the magnetic field produced by these current strip using the Faraday effect. The experimental set up is shown in the Fig. 8. Results of the measurement is shown in Fig. 9. The residual field decays down to 0.1 ppm level 20 μ-sec. after the kicker firing.

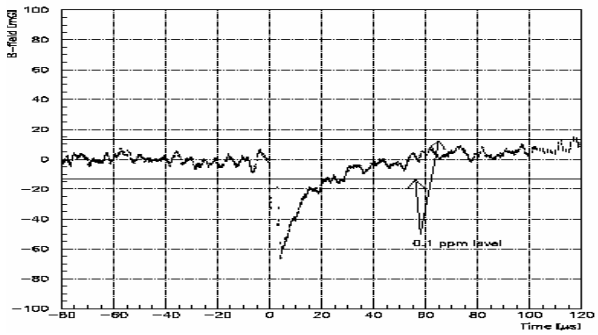

Fig. 9: Kicker residual field vs. time after the kicker firing, time scale is 20 μ-sec. per box. The horizontal line indicates 0.1 ppm effect.

5 MESUREMENT RESULT

The frequency ω_a is obtained from the time distribution of decay e+ counts. The e+ are detected by calorimeters whose photomultiplier signals have a typical FWHM of 5ns. The signals are sampled every 2.5 ns by waveform digitizers (WFD) with at least 16 samples per e+ event. The samples are used to determine e+ times and energies, and for pulse overlap studies. The pulse reconstruction algorithm fits signals above baseline to an average pulse shape, determined for each calorimeter individually. Multiple pulses can be resolved if their separation exceeds 3 to 5 ns. Systematic effects associated with the algorithm were extensively studied. Detailed study of the systematic studies are done. They are (1) e+ pulses overlapping in time (pileup), (2) coherent betatron oscillations, (3) beam debunching, (4) muon losses, and (5) detector gain stability during the muon storage time. Resulting positron time spectrum is shown in Fig. 10. Summary of systematic error given in Table 2. A summary of total experimental error is given in the Table 3.

Table 2:
Systematic error for ω_a

	ppm
Gain Instability	0.02
Events Pileup	0.13
Coherent Betatron Motion	0.05
Lost Muons	0.10
Timing shifts	0.10
Vertical Orbit and E Field	0.08
Binning	0.07
Beam Debunching	0.04
AGS background	0.10
Total	0.25

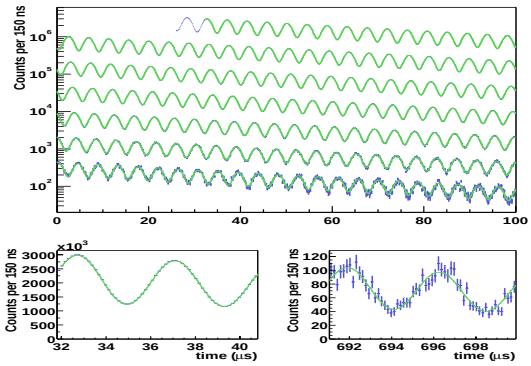

Fig. 10: Positron time spectrum with the first and the last two cycles in bottom figures.

Table 3:
Error Summary

	ppm
Statistical	1.25
Systematic ω_p	0.40
Systematic ω_a	0.25
Total	1.34

The resulting a_μ is

$$a_\mu^{EXP} = 116\ 592\ 03(15) \times 10^{-10} \quad (1.3\ ppm)$$

Compared to most recent theoretical value based on the Standard Model

$$a_\mu^{SM} = 116\ 591\ 596(67) \times 10^{-10} \quad (0.6\ ppm)$$

The a_μ^{EXP} and a_μ^{SM} are 2.6 standard deviation apart, and implication, provided no mistake in experiment, may be SUSY or other physics.

We thank T. Kirk, D.I. Lowenstein, P. Pile, and the staff of the BNL AGS for the strong support they have given this experiment. We thank D. Cassel, A. Czarnecki, M. Davier, T. Kinoshita, W. Marciano, and J. Urheim for helpful discussions.

REFERENCES

[1] J. Bailey *et al.*, Nucl. Phy. B150, 1 (1979)
[2] R.N. Brown *et al.*, Muon *(g* -2) Collaboration, Phys. Rev. D62, 091101 (2000).
[3] R.M. Carey *et al.*, Muon *(g* -2) Collaboration, Phys. Rev. Lett. 82, 1632 (1999).
[4] F. Krienen *et al.*, Nucl. lustrum. Methods A283, 5 (1989). A. Yamarnoto *et at.*, Proc. of 15th Int. Conf. on Magnet Tech., Science Press Beijing, 246 (1998).
[5] G.T. Danby, *et al.*, Nucl. Instrum. Methods A457, 151 (2001).
[6] R. Prigl *et at.*, Nucl. Instrum. Methods A374, 118 (1996)
[7] S. Sedykh *et at.*, Nucl. Instrum. Methods A455, 346 (2000).